

Effects of ultrasonic treatment on microstructures of AZ91 alloy

Yue-shuang YANG¹, Jin-cheng WANG¹, Tao WANG¹, Cheng-ming LIU¹, Zhong-ming ZHANG²

1. State Key Laboratory of Solidification Processing, Northwestern Polytechnical University, Xi'an 710072, China;

2. School of Materials Science and Engineering, Xi'an University of Technology, Xi'an 710048, China

Received 23 October 2012; accepted 15 March 2013

Abstract: Effects of ultrasonic treatment on microstructures were investigated by introducing the ultrasonic oscillation into AZ91 alloy melts. The results show that the ultrasonic treatment does not change the phase composition but has great influence on solidification microstructures. The area percentage of lamellar eutectic phase increases to the maximum when the applied ultrasonic power is increased to 600 W and then decreases gradually with the further increase of power; meanwhile, the average area of Al_8Mn_5 phase owns a completely opposing variation trend. The area percentage of $\text{Mg}_{17}\text{Al}_{12}$ decreases gradually with increasing the applied ultrasonic power. Mechanisms accounted for the refinement and fraction of different intermetallic phases were also discussed.

Key words: AZ91 alloy; ultrasonic treatment; microstructure

1 Introduction

Magnesium alloys have excellent potentials to be used as structure materials in automotive, electronics and aerospace fields due to their interesting combination of engineering properties such as low density, excellent machinability and good damping capacity [1–4]. The most widely used Mg alloy is AZ91 alloy. However, its strength and ductility are still not good enough for more widely commercial applications. Grain refinement is routinely practised in material processing and has decisive effects on the microstructures and properties of castings.

Achieving fine and equiaxed grain structures is a central task of solidification processing, which has thus been an important topic in solidification. It can be carried out through many different methods, among which the most familiar one is inoculation. Although Al-free Mg alloys can be readily refined by Zr, it has been proved that the more common Mg–Al based commercial alloys are difficult to be refined by inoculation [5]. As an alternative, ultrasonic treatment (UST) has shown significant potentials for grain refinement of Mg–Al based alloys [6,7].

UST is a relatively new and effective technology [8–10]. The introduction of powerful ultrasonic oscillations into melts can be quite simply adapted to the industrial smelting process. In practice, ultrasonic oscillations can be directly introduced into solidifying melts via an immersed sonotrode or indirectly through the non-contact approach, depending on the melting point and its chemical reactivity with the sonotrode [11]. For ultrasonication of low melting point alloys such as Mg and Al alloys, the direct approach is preferred due to the fact that the ultrasonic energy can be efficiently introduced into the melts for effective ultrasonication.

Previous experiments on Mg alloys have shown a promising effect of ultrasonic oscillations on grain refinement. Several different mechanisms that may be responsible for the microstructure refinement also have been proposed [12,13]. However, almost all researches only reported the influence of UST on structure characteristics of primary α -Mg phase [14,15], but very little information on the intermetallic phases which are formed during solidification is available. For Mg alloys containing Al and Mn, these phases may include $\text{Mg}_{17}\text{Al}_{12}$ and Al_8Mn_5 phases [16,17]. AGHAYANI and NIROUMAND [18] found that applying ultrasonic oscillations into melts prior to casting had a significant

Foundation item: Project (51071128) supported by the National Natural Science Foundation of China; Project (2011CB610401) supported by the National Basic Research Program of China; Project (SKLSP201002) supported by Free Research Fund of State Key Laboratory of Solidification Processing, China

Corresponding author: Jin-cheng WANG; Tel: +86-29-88460650; Fax: +86-29-88491484; E-mail: jchwang@nwpu.edu.cn
DOI: 10.1016/S1003-6326(14)63030-2

effect on the size, continuity, sphericity and distribution of $Mg_{17}Al_{12}$ phase, and believed that increasing the applied ultrasonic power can generate much smaller, more rounded and better distributed $Mg_{17}Al_{12}$ phase. As to the Al_8Mn_5 phase, however, little work has been done. Therefore, in the present work, we focus on the effect of UST on the microstructures of AZ91 alloy, especially on the two intermetallic phases. The mechanisms of microstructure modification are also discussed.

2 Experimental

The composition of AZ91 alloy used in this work was $Mg-9Al-0.65Zn-0.35Mn$ and the melting process was carried out in an electrical resistance furnace under an atmosphere containing a gas mixture of CO_2 and SF_6 . A stainless steel crucible was employed, and a thermocouple was inserted near the middle of the melt to acquire the temperature during solidification. Schematic diagram of the experiment apparatus is shown in Fig. 1.

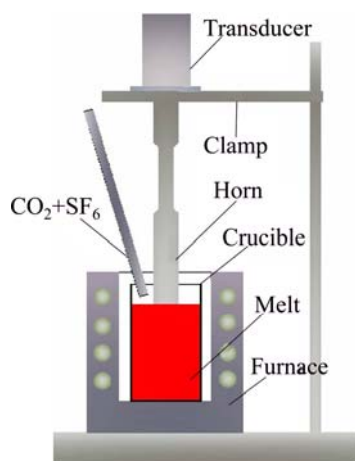


Fig. 1 Schematic diagram of experimental apparatus

The ultrasonic oscillation system consisted of an acoustic generator with a maximum power of 3 kW, a transducer with a frequency of 20 kHz and a titanium ultrasonic horn. The melt was modified with C_2Cl_6 and purified with Ar_2 respectively at 745 °C and then cooled down to 720 °C. Ultrasonic horn was quickly immersed into the melt to be preheated and the melt was cooled down to 680 °C where it was isothermally subjected to continuous oscillations for 100 s. Then the ultrasonic horn was quickly removed and the melt was poured into a preheated metal mould. In order to compare the microstructures of the various specimens processed under different ultrasonic powers, the melt was treated by ultrasonic oscillations with powers of 0 (no ultrasonic treatment), 400, 600, 800 and 1000 W, respectively. The samples were cut at the same location for comparison.

As-cast samples were then sectioned, ground, polished and etched with a solution of 1% nitric acid in

alcohol to reveal their microstructures. Microstructure characterization was identified by laser scanning confocal microscope, X-ray diffraction and scanning electron microscope. Both the average grain size of Al_8Mn_5 particles and the percentage of $Mg_{17}Al_{12}$ phase and eutectic phase were measured by image analysis software named Image J.

3 Results

3.1 Microstructures

Figure 2 shows the representative microstructures of as-cast AZ91 alloy without and with UST. For the alloy with UST, the treatment time is 100 s and the power is 600 W. In the alloy without UST, as shown in Fig. 2(a), the matrix consists of equiaxed grains of primary phase with the equivalent diameter of about 125 μm and some dot-like particles are distributed in the grains. As to the microstructure of as-cast AZ91 alloy with UST, it is very similar to that without UST, especially the phase compositions. The volume fraction of grain boundary and phases appearing along the grain boundary are

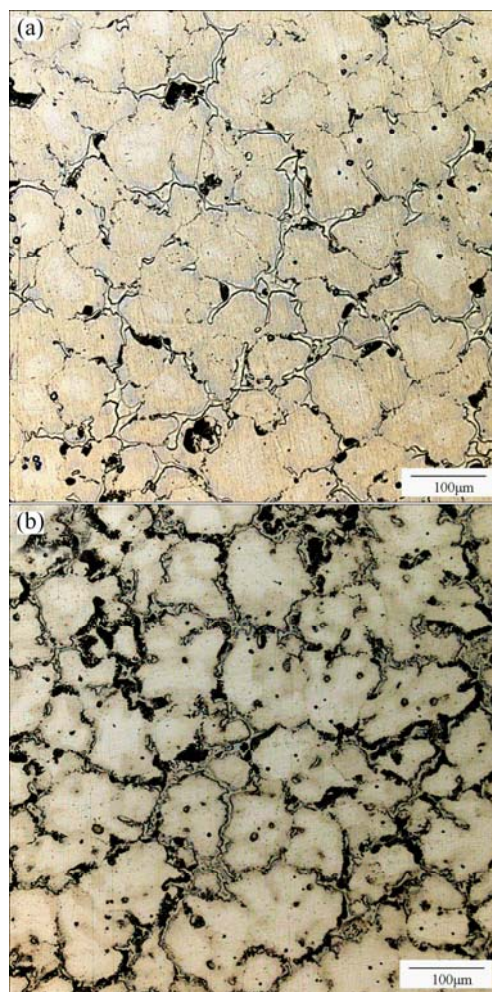


Fig. 2 Laser scanning confocal microscope (LSCM) images of as-cast AZ91 alloys without (a) and with UST (b)

slightly increased, which results in the equivalent diameter of grains decreasing slightly to about 98 μm . In addition, dot-like particles in the grain and phases along the grain boundary are distributed more uniformly compared with those without UST.

To show microstructures of the as-cast sample with UST more clearly, SEM image of the as-treated sample by ultrasonic oscillations at 600 W is shown in Fig. 3. Four types of phases could be detected in the as-cast microstructure clearly: black matrix phase, white dot-like phase distributed in the matrix, grey netted shape phase and lamellar eutectic phase along the grain boundaries. According to the phase diagram [16], the matrix phase is the primary phase α -Mg, while the eutectic phase should be composed of α -Mg and $\text{Mg}_{17}\text{Al}_{12}$. To identify the other two phases (as marked in Fig. 3 by *A* and *B*), XRD and TEM experiments were conducted to analyze these phases. The result of XRD analysis shown in Fig. 4 indicates that the microstructures are composed of α -Mg, $\text{Mg}_{17}\text{Al}_{12}$ and Al_8Mn_5 . Table 1 presents the compositions of the phases marked in Fig. 3 which were obtained by EDS. Figure 5 shows the electron diffraction patterns of these two phases. All the results identify that the white dot-like phase distributed in the matrix (phase *A*) and the grey netted shape phases along the grain boundaries

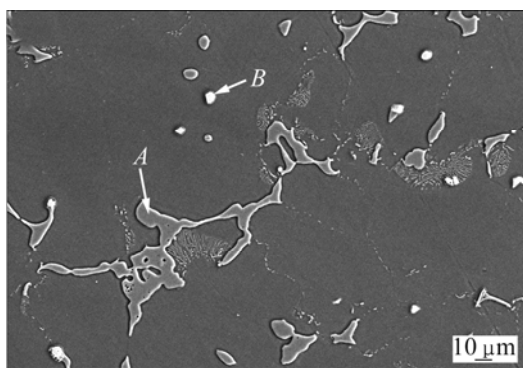


Fig. 3 SEM image of AZ91 alloys with UST

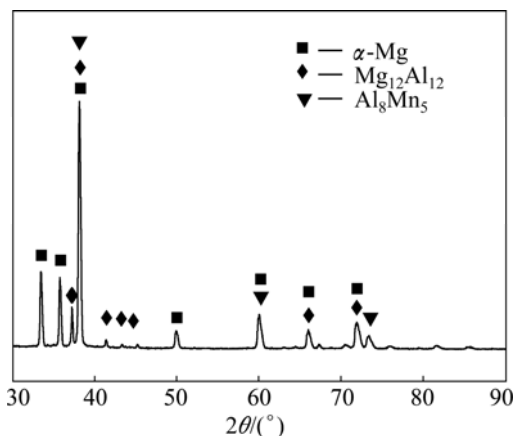


Fig. 4 XRD pattern of AZ91 alloys with UST

Table 1 Results of EDS analysis of different phases marked in Fig. 3

Point	$x(\text{Mg})/\%$	$x(\text{Al})/\%$	$x(\text{Zn})/\%$
<i>A</i>	62.77	35.53	1.59
<i>B</i>	10.97	51.72	37.81

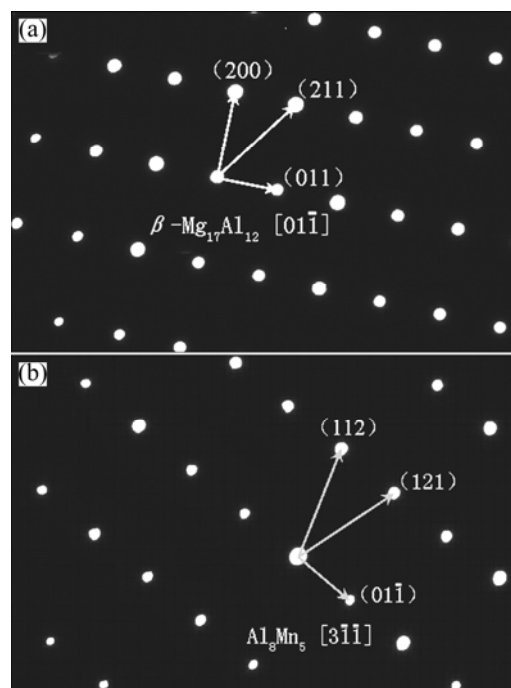


Fig. 5 Electron diffraction patterns of AZ91 alloys with UST: (a) $\text{Mg}_{17}\text{Al}_{12}$; (b) Al_8Mn_5

(phase *B*) should be $\text{Mg}_{17}\text{Al}_{12}$ and Al_8Mn_5 respectively, which is in accordance with result in Refs. [16,17].

3.2 Effect of ultrasonic power on microstructures

Figure 6 shows the SEM images of AZ91 alloy treated with different ultrasonic powers. It shows that, with the increase of the applied UST power, the phase composition does not change but the size, fraction and distribution of the intermetallic phases change remarkably. Effects of the applied UST power on the area percentages of $\text{Mg}_{17}\text{Al}_{12}$ phase and lamellar eutectic phase as well as the average area of Al_8Mn_5 particles are shown in Fig. 7. Figure 7(a) indicates that the area percentage of lamellar eutectic phase increases to the maximum when the applied UST power is increased to 600 W and then the percentage decreases gradually with the further increase of UST power. However, the area percentage of $\text{Mg}_{17}\text{Al}_{12}$ decreases with the applied UST power constantly. Figure 7(b) shows that the average area of Al_8Mn_5 particles reduces from 16.38 to 10.32 μm^2 when the applied UST power increased from 0 to 600 W. However, the grain area increases rapidly to 25.96 μm^2 when the power is further increased to 1000 W.

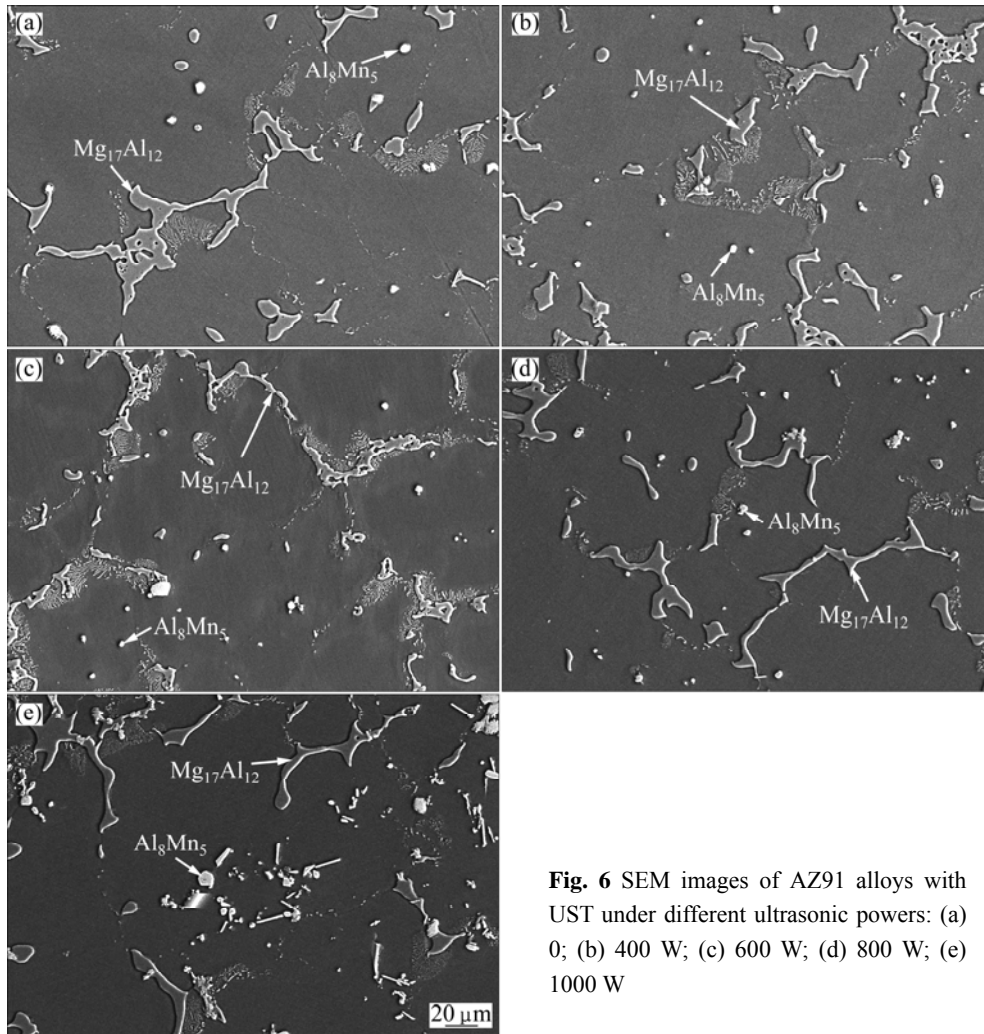


Fig. 6 SEM images of AZ91 alloys with UST under different ultrasonic powers: (a) 0; (b) 400 W; (c) 600 W; (d) 800 W; (e) 1000 W

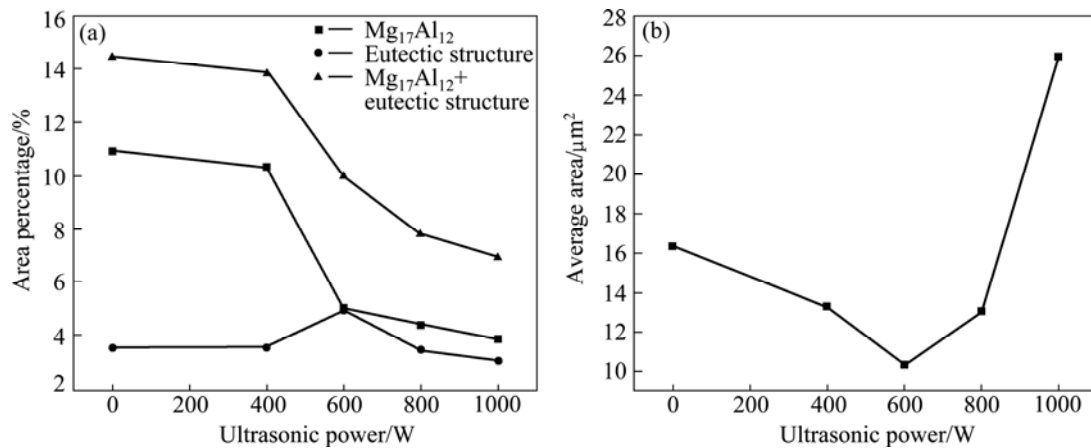


Fig. 7 Effect of applied ultrasonic power on area percentage of Mg₁₇Al₁₂ and eutectic phase (a) and average area of Al₈Mn₅ particles (b)

4 Discussion

Grain size of solidification microstructures is mainly dependent on the heterogeneous nucleation process and subsequent growth condition of the newly

formed nuclei. The sufficient number of nuclei and applicable temperature for the survival of nuclei are essential to the grain refinement. When the melts are subjected to high-intensity ultrasonic oscillations, the cavitations and streaming phenomena will take place and instantaneous pressure and temperature fluctuations in

the melts may be induced by the cavitations.

The instantaneous temperature and pressure induced by cavitations can be calculated by [19]

$$T = T_0 \left[\frac{p_m(\gamma - 1)}{p_0} \right] \quad (1)$$

$$p = p_0 \left[\frac{p_m(\gamma - 1)}{p_0} \right]^{\frac{\gamma}{\gamma - 1}} \quad (2)$$

where T_0 is the temperature of melt, p_m is the pressure amplitude of ultrasonic, p_0 is the hydrostatic pressure and γ is the specific heat coefficient. The relationship between pressure and temperature for the phase change boundaries can be described by Clausius–Clapeyron relation, i.e.,

$$\frac{dp}{dT} = \frac{\Delta H}{T(V_G - V_L)} \quad (3)$$

where dp/dT is the slope of the coexistence curve, ΔH is the latent heat, T is the temperature, and $V_G - V_L$ is the volume change during the phase transition.

In this work, UST was applied at 680 °C which is about 20 °C higher than the melting point (660 °C) of Al_8Mn_5 phase. Few Al_8Mn_5 grains are expected to form at this temperature. However, it has been shown that cavitations may generate instantaneous pressure pulses with the order of 100–1000 MPa [6]. A simple calculation using Clausius–Clapeyron equation and thermo-physical properties of molten Mg shows that the melting point of the alloy can increase by 12–120 °C under such pressures [18]. In the case of Al_8Mn_5 phase, considerable local undercooling will be generated under the instantaneous pressure pulses because of the remarkable increase of the melting point. Under the effect of acoustic streaming, quantities of Al_8Mn_5 nuclei are developed and distributed uniformly. Meanwhile, a high proportion of nuclei is expected to survive after UST due to the small gap between UST temperature and liquidus temperature. The number of survived nuclei increases and the size of Al_8Mn_5 phase decreases gradually with increase of the ultrasonic power. The instantaneous pressure and temperature pulses induced by the collapse of bubbles play an opposing role in the process of nucleation. The temperature pulses could melt the nuclei which were nucleated due to the pressure pulses. Therefore, when the ultrasonic power exceeds 600 W, the localized temperature pulses play a more important role compared with the localized pressure pulses; thus with the applied power further increasing, coarse Al_8Mn_5 phase appears again.

As to the α -Mg phase, the gap between treating temperature and melting point (600 °C) of the α -Mg phase is very large; moreover, the instantaneous pressure pulses are transient. So, the α -Mg particles cannot

survive after the instantaneous pressure disappears or during the interval between the cessation of UST and pouring of the melts into the mould. As a result, the cavitations under UST appear to be very limited for the refinement of the α -Mg grains.

The melting point of the $Mg_{17}Al_{12}$ phase is 460 °C, which is about 220 °C below the UST temperature. No such a high undercooling is expected to generate under the instantaneous pressure pulses. Therefore, the main mechanism for this phase is acoustic streaming. During the process of non-equilibrium solidification, the element Al accumulates at the grain boundaries and the concentration increases to the hypoeutectic area gradually along with the α -Mg phase precipitated [20]. Therefore, nodular $Mg_{17}Al_{12}$ phase and lamellar eutectic structure appear at the grain boundaries. The acoustic stream induced by ultrasound oscillations decreases the boundary segregation of Al. Based on this, the concentration at the boundaries decreases gradually with the applied UST power. According to the lever rule, the percentage of $Mg_{17}Al_{12}$ structure decreases with the concentration correspondingly. When the power is increased to 600 W, the concentration approaches gradually to the eutectic point and the area percentage of lamellar eutectic phase increases to the maximum. With further increasing the power, the fraction of eutectic phase decreases gradually.

5 Conclusions

1) AZ91 alloy consists of matrix α -Mg phase, dot-like Al_8Mn_5 phase in matrix, black nodular $Mg_{17}Al_{12}$ phase and netted shape eutectic structure at grain boundaries. The equivalent diameter of α -Mg phase can be modified from 125 to 98 μm with the application of ultrasonic vibration.

2) The average area of Al_8Mn_5 particles decreases to the minimum when the applied ultrasonic power is increased to 600 W and then increases rapidly with the further increase of ultrasonic power. The microstructure modifications are mainly attributed to the acoustic cavitations.

3) The area percentage of $Mg_{17}Al_{12}$ decreases gradually with increasing the applied ultrasonic power. The fraction change is mainly attributed to the acoustic streaming by reducing the boundary segregation of Al.

References

- [1] MORDIKE B L, EBERT T. Magnesium: Properties–applications–potential [J]. Materials Science and Engineering A, 2001, 302(1): 37–45.
- [2] FRIENDRICH H, SCHUMANN S. Research for a “new age of magnesium” in the automotive industry [J]. Journal of Materials Processing Technology, 2001, 117(3): 276–281.

- [3] SCHUMANN S. The paths and strategies for increased magnesium applications in vehicles [J]. Materials Science Forum, 2005, 488–489(1): 1–8.
- [4] KULEKCI M K. Magnesium and its alloys applications in automotive industry [J]. International Journal of Advanced Manufacturing Technology, 2008, 39(9–10): 851–865.
- [5] STJOHN D H, QIAN M, EASTON M A, CAO P, HILDEBRAND Z. Grain refinement of magnesium alloys [J]. Metallurgical and Materials and Transaction A, 2005, 36(7): 1669–1679.
- [6] ESKIN G I. Ultrasonic treatment of light alloy melts [M]. Amsterdam: Gordon & Breach, 1998.
- [7] ABRAMOV O V. Ultrasound in liquid and solid metals [M]. Boca Raton, FL: CRC, 1994: 289–329.
- [8] ESKIN G I. Broad prospects for commercial application of the ultrasonic (cavitation) melt treatment of light alloys [J]. Ultrasonics Sonochemistry, 2001, 8(3): 319–325.
- [9] YAO Lei, HAO Hai, JI Shou-hua, FANG Can-feng, ZHANG Xing-guo. Effects of ultrasonic vibration on solidification structure and properties of Mg–8Li–3Al Alloy [J]. Transactions of Nonferrous Metals Society of China, 2011, 21(6): 1241–1246.
- [10] ZHANG Hai-bo, ZHAI Qi-jie, QI Fei-peng, GONG Yong-yong. Effect of side transmission of power ultrasonic on microstructure of AZ81 magnesium [J]. Transactions of Nonferrous Metals Society of China, 2004, 14(2): 302–305. (in Chinese)
- [11] QIAN M, RAMIREZ A, DAS A. Ultrasonic refinement of magnesium by cavitation: Clarifying the role of wall crystals [J]. Journal of Crystal Growth, 2009, 311(14): 3708–3715.
- [12] ESKIN G I. Influence of cavitations treatment of melts on the processes of nucleation and growth of crystals during solidification of ingots and castings from light alloys [J]. Ultrasonics Sonochemistry, 1994, 1(1): S59–S63.
- [13] ABRAMOV V, ABRAMOV O, BULGAKOV V, SOMMER F. Solidification of aluminum alloys under ultrasonic irradiation using water-cooled resonator [J]. Materials Letters, 1998, 37(1): 27–34.
- [14] LIU X B, OSAWA Y, TAKAMORI S, MUKAI T. Grain refinement of AZ91 alloy by introducing ultrasonic oscillations during solidification [J]. Materials Letters, 2008, 62(3): 2872–2875.
- [15] LIU X B, OSAWA Y, TAKAMORI S, MUKAI T. Microstructure and mechanical properties of AZ91 alloy produced with ultrasonic oscillations [J]. Materials Science and Engineering A, 2008, 487(1–2): 120–123.
- [16] LIU Chu-ming, ZHU Xiu-rong, ZHOU Hai-tao. Phase diagrams of magnesium alloys [M]. Changsha: Central South University of Technology Press, 2006. (in Chinese)
- [17] SIN S L, DUBE D, TREMBLAY R. Characterization of Al–Mn particles in AZ91D investment castings [J]. Materials Characterization, 2007, 58(10): 989–996.
- [18] AGHAYANI K M, NIROUMAND B. Effects of ultrasonic treatment on microstructure and tensile strength of AZ91 magnesium alloy [J]. Journal of Alloys and Compounds, 2011, 509(1): 114–122.
- [19] FENG Nuo. Ultrasound handbook [M]. Nanjing: Nanjing University Press, 1999: 83–88. (in Chinese)
- [20] ZHANG Z Q, LE Q C, CUI J Z. Influence of high-intensity ultrasonic treatment on the phase morphology of a Mg–9.0 wt.% Al binary alloy [J]. Rare Metals, 2009, 28(1): 86–90.

超声处理对 AZ91 合金微观组织的影响

杨跃双¹, 王锦程¹, 王 陶¹, 刘成明¹, 张忠明²

1. 西北工业大学 凝固技术国家重点实验室, 西安 710072;

2. 西安理工大学 材料学院, 西安 710048

摘 要: 通过在 AZ91 合金熔体中引入超声振动研究超声处理对合金微观组织的影响。结果表明, 超声处理并不改变合金的相组成, 但对凝固组织有显著影响; 随着超声功率的增加, 层片状共晶组织的面积分数呈现先增加后降低的趋势, 当超声功率为 600 W 时达到最高, 而 Al_8Mn_5 相的平均面积变化规律则完全相反, $\text{Mg}_{17}\text{Al}_{12}$ 相的面积分数则随着超声功率的增加而逐渐降低。讨论了组织细化及相分数改变的超声处理机制。

关键词: AZ91 合金; 超声处理; 微观组织

(Edited by Xiang-qun LI)